ЖУРНАЛ СТРУКТУРНОЙ ХИМИИ

2012. Том 53, № 4 *Июль – август* *С. 687 – 695*

UDC 541.6:546.171:547.23

A DFT STUDY ON THE STRUCTURE AND DETONATION PROPERTIES OF AMINO, METHYL, NITRO, AND NITROSO SUBSTITUTED 3,4,5-TRINITROPYRAZOLE-2-OXIDES: NEW HIGH ENERGY MATERIALS

P. Ravi[1], G.M. Gore[2], A.K. Sikder[2], S.P. Tewari[1]

[1]*Advanced Centre of Research in High Energy Materials (ACRHEM), University of Hyderabad, P.O. Central University, Hyderabad, India,* e-mail: rpiitb@hotmail.com, ak_sikder@yahoo.com
[2]*High Energy Materials Research Laboratory (HEMRL), Pune, India*

Received January, 24, 2011

The structure, band gap, thermodynamic properties and detonation properties of methyl, amino, nitro, and nitroso substituted 3,4,5-trinitropyrazole-2-oxides are explored using density functional theory at the B3LYP/aug-cc-pVDZ level. It is found that the NH_2 or CH_3 group substitution for the acidic proton at the N4 position of trinitropyrazole-2-oxide (**P20**) decreases the heat of detonation and crystal density. The density (2.20—2.50 g/cm^3), detonation velocity (10.20—10.92 km/s), and detonation pressure (52.30—59.84 GPa) of the title compounds are higher compared with 1,3,5,7-tetranitro-1,3,5,7-tetrazocine (HMX), 2,4,6,8,10,12-hexanitro-2,4,6,8,10,12-hexaazaisowurtzitane (CL-20), and octanitrocubane (ONC).

Keywords: 3,4,5-trinitropyrazole-2-oxides, density, detonation performance, impact sensitivity.

INTRODUCTION

Due to their positive heat of formation, good thermal stability, higher density and better detonation performance nitropyrazoles have been receiving renewed attention by explosives chemists [1]. Dinitropyrazoles in which two or three NO_2 groups attached to ring carbon atoms are known [2]. 3,4,5-Trinitro-1H-pyrazole (**TNP**) is a non-hygroscopic, weakly acidic, insensitive, and exceptionally stable all C-nitrated compound [3—6]. The heat of decomposition of **TNP** is 255 J/g, which is extremely low for a high energy compound. It is known that the substitution of labile hydrogen of 3,4,5-trinitro-1H-pyrazole by NO, NO_2, NH_2 and CH_3 groups enhances the performance properties [1]. Furthermore, the presence of N-oxide bonds in the aromatic N-heterocycles increases the heat of formation, crystal density, and thus, the detonation performance [7]. To our knowledge, there were no such studies on the structure and explosive properties of trinitropyrazole-2-oxides. Thus, it would be desirable before attempting their synthesis to be able to predict the heat of detonation, density, detonation performance, stability and sensitivity.

The sensitivity of explosives has been related to the molecular and electronic structures and the properties of energetic R—NO_2 (where, R = C, N and O) bonds such as electrostatic potentials, lengths and bond energy [7—9]. Pospìŝil [10] correlated the crystal volume to the impact sensitivity. Zhang et al [11, 12] correlated the electronic structure to the impact sensitivity by NO_2 group charge analysis. Zeman [13] related the impact and electric spark sensitivities to detonation and thermal decomposition, ^{13}C NMR and ^{15}N NMR chemical shifts. Electric spark sensitivity (E_{ES}) was related to the squares of detonation velocity and reciprocal temperature, the Piloyan activation energy, and heats of fusion [14]. Zhi and Cheng [15] shown the relationship between the electric spark sensitivity, lowest unoccupied molecular orbital energy, Mulliken charge of the nitro group, the number of aromatic rings, and the number of substituents attached to the aromatic ring. The stability of model compounds have been evaluated from the nitro group charge analysis and the frontier molecular orbital energy gaps [16, 17].

In the present study, density functional theory (DFT) calculations at the B3LYP/aug-cc-pVDZ level have been carried out to investigate the geometry, band gap, heat of detonation, crystal density, detonation velocity, detonation pressure, stability, impact sensitivity ($H_{50\,\%}$) and electric spark sensitivity (E_{ES}) of nitroso-3,4,5-trinitropyrazole-2-oxide (**P24**), 1-amino-3,4,5-trinitropyrazole-2-oxide (**P21)**, 1-methyl-3,4,5-trinitropyrazole-2-oxide (**P22**), 1,3,4,5-tetranitropyrazole-2-oxide (**P23**), and 1-nitroso-3,4,5-trinitropyrazole-2-oxide.

METHODS AND CALCULATION DETAIL

Density functional theory (DFT) calculations were carried out for the model compounds using the Gaussian 03 program [18]. The molecules were optimized at the B3LYP/aug-cc-pVDZ level knowing the method and basis set that give better approximations [7]. All the stationary points have been identified as local minima with no imaginary frequencies. The optimized structures were then used to determine the densities (ρ) using the Material Studio 4.1 package [19] with cvff and the Ewald summation method.

The chemical energies of detonation ($\Delta H_{298.15\text{ K}}$ or Q) for the compounds were calculated using the following expression:

$$Q \text{ (or) } \Delta H_{298.15\text{ K}} = \Delta E_{298.15\text{ K}} + \Delta(PV) = \Delta E_0 + \Delta\text{ZPE} + \Delta_T H + \Delta nRT, \qquad (1)$$

where ΔE_0 is the change in total energy between the products and the reactants at 0 K; ΔZPE is the difference between the zero point energies (ZPEs) of the products and reactants; $\Delta_T H$ is the difference between the thermal correction from 0 to 298.15 K of the products and reactants; $\Delta(PV)$ equals to ΔnRT for the reaction of ideal gases, $\Delta n = 0$. The Kamlet and Jacob equations were used to determine the performance properties [20]

$$P = 15.58\text{NM}^{1/2}Q^{1/2}\rho^2 \qquad (2)$$

$$D = 1.01(\text{NM}^{1/2}Q^{1/2})^{1/2}(1 + 1.30\rho), \qquad (3)$$

where P is the detonation pressure in GPa, D is the detonation velocity in km/s, N is the number of moles of gaseous detonation products per gram of explosive, M is the average molecular weight of the gaseous products, Q is the energy of explosion in kcal/g of explosive, and ρ is the density in g/cm^3. The possible detonation products of designed compounds have been written based on the modified Kistiakowsky—Wilson rules [21].

$$C_3HN_5O_7 \rightarrow 3CO_2 + \frac{1}{2}H_2O + 2\frac{1}{2}N_2 + \frac{1}{4}O_2\ (\mathbf{P20}), \qquad (4)$$

$$C_3H_2N_6O_7 \rightarrow 3CO_2 + H_2O + 3N_2\ (\mathbf{P21}), \qquad (5)$$

$$C_4H_3N_5O_7 \rightarrow 2\frac{1}{2}CO + 1\frac{1}{2}CO_2 + 1\frac{1}{2}H_2O + 2\frac{1}{2}N_2\ (\mathbf{P22}), \qquad (6)$$

$$C_3N_6O_9 \rightarrow 3CO_2 + 3N_2 + 1\frac{1}{2}O_2\ (\mathbf{P23}), \qquad (7)$$

$$C_3N_6O_8 \rightarrow 3CO_2 + 3N_2 + O_2\ (\mathbf{P24}). \qquad (8)$$

Mulliken charges have been used to evaluate the stability and sensitivity of the designed molecules, knowing that the Mulliken charges are qualitatively correct and reproducible for a basis set. The nitro group ($—Q_{NO_2}$) charge has been calculated by the sum of the net Mulliken atomic charges on nitrogen (Q_N) and oxygen atoms (Q_{O1} and Q_{O2}) of the NO_2 group [11, 12]. We have also predicted the electric spark sensitivity from the nitro group ($—Q_{NO_2}$) charge and the lowest unoccupied molecular orbital (LUMO) of the molecule. The stability has been determined from the total energy as well as from the frontier molecular orbital energy gaps [15].

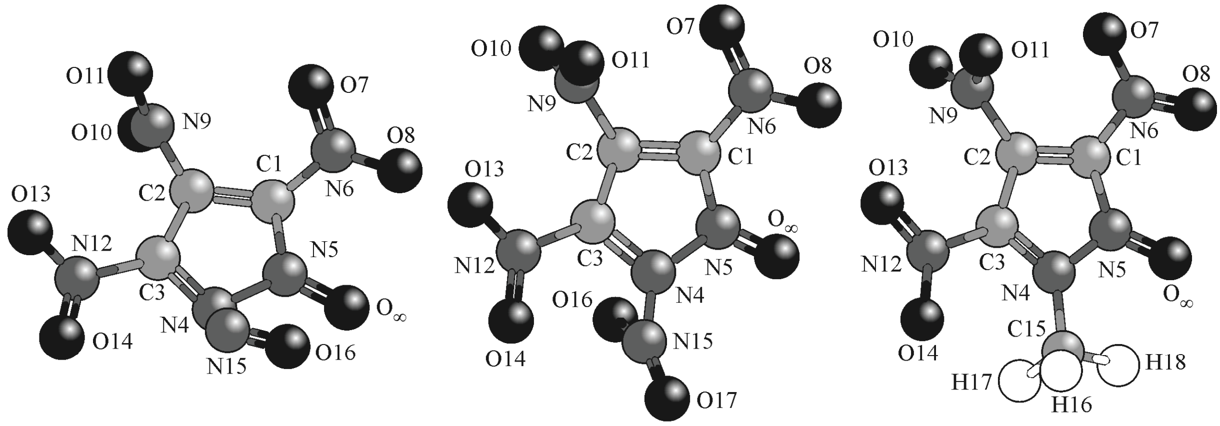

P24 **P23** **P22**

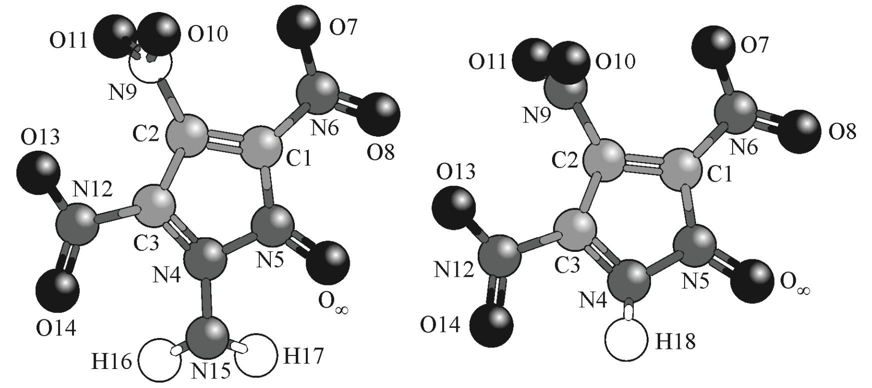

P21 **P20**

Fig. 1. Computed structures of model molecules

RESULTS AND DISCUSSION

Optimized structures. We have optimized the structures at the B3LYP/aug-cc-pVDZ level, and the optimized structures are shown in Fig. 1. The selected structural parameters of the optimized structures at the B3LYP/aug-cc-pVDZ level are listed in Table 1. In 3,4,5-trinitropyrazole-2-oxide (**P20**), the two nitro groups (N6O7O8 and N12O13O14) and amino hydrogen form the molecular plane, however, the nitro oxygen (O10 and O11) atoms of C2—NO$_2$ are rotated by about ± 35.5° from the molecular plane. It is due to the repulsion between the neighboring nitro groups rotating the oxygen atoms of C2—NO$_2$ from the molecular plane. The interatomic O7···O11 and O13···O10 distances in **P20** are 3.194 Å and 3.328 Å respectively. The bond lengths of C1—NO$_2$, C2—NO$_2$, and C3—NO$_2$ in **P20** are 1.438 Å, 1.471 Å, and 1.428 Å respectively. Amino nitrogen (N15) of the 1-amino-3,4,5-trinitropyrazole-2-oxide (**P21**) molecule deviates from the molecular plane by 9.06°. The interatomic H16···O14 distance is 2.308 Å, a typical distance of the N—H···O hydrogen bond [22]. The nitro oxygen (O14) atom of the C3—NO$_2$ group shows the deviation from the molecular plane by about 8.5°. This rotation makes the O14 oxygen atom of the NO$_2$ group close to that of H16 amino hydrogen facilitating a strong intramolecular N—H···O hydrogen bond. The interatomic O7···O11 and O13···O10 distances in **P21** are 3.243 Å and 3.285 Å respectively. The bond lengths of C1—NO$_2$, C2—NO$_2$, and C3—NO$_2$ in **P21** are 1.438 Å, 1.471 Å, and 1.428 Å respectively. In 1-methyl-3,4,5-trinitropyrazole-2-oxide (**P22**), the C15···O14 length is 2.813 Å, which is the C···O interaction. The interatomic distances of O7···O11 and O13···O10 in **P22** are 3.173 and 3.188 Å respectively. The bond lengths of C1—NO$_2$, C2—NO$_2$ and C3—NO$_2$ in **P22** are 1.440 Å, 1.470 Å, and 1.433 Å respectively. The interatomic O14···N15 distance in 1,3,4,5-tetranitropyrazole-2-oxide (**P23**) is 2.832 Å, which is the N···O type interaction. The interatomic O7···O11 and O13···O10 distances in **P23** are 3.186 Å and 3.302 Å respectively. The bond lengths of C1—NO$_2$, C2—NO$_2$, C3—NO$_2$ and N4—NO$_2$

Table 1

Selected structural parameters[a] *of model compounds*

Parameter	**P20**	**P21**	**P22**	**P23**	**P24**
C1—C2	1.411	1.401	1.403	1.420	1.410
C2—C3	1.374	1.383	1.377	1.367	1.383
C3—N4	1.370	1.376	1.378	1.390	1.362
N4—N5	1.362	1.365	1.380	1.413	1.375
N5—C1	1.382	1.383	1.377	1.366	1.380
N6—C1	1.438	1.438	1.440	1.440	1.437
N9—C2	1.470	1.471	1.470	1.472	1.468
N12—C3	1.428	1.430	1.433	1.434	1.438
N15—N4	1.016	1.388	1.464	1.596	1.602
N5—O§	1.236	1.247	1.240	1.230	1.250
N15—H16		1.020	1.093		
N15—H17		1.026	1.093		
O7…N9	2.814	2.818	2.801	2.810	2.830
O13…N9	2.956	2.891	2.814	2.901	2.901
O14…N15				2.832	3.240
C1—C2—C3	106.5	107.0	106.6	107.0	106.0
N4—C3—C2	108.0	107.7	108.8	107.2	106.1
N5—N4—C3	110.5	109.7	108.5	107.3	110.1
N4—N5—C1	106.3	107.1	107.5	118.7	100.2
N15—N4—N5	120.0	117.4	119.2		
O§—N4—N5	121.6				
O7—N6—O8	127.0	126.8	127.0	127.1	126.6
O10—N9—O11	128.1	128.0	128.0	128.4	128.0
O13—N12—O14	127.0	126.3	126.2	127.0	126.4
H16—N15—N4		108.1	109.6	112.7	109.2
H17—N15—N4		105.0		112.4	
H18—C15—N4			105.8		
C1—C2—C3—N4	0	1.28	0	–4.7	2.0
C2—C3—N4—N5	0	1.84	0	8.4	–1.6
C3—N4—N5—C1	0	1.65	0	–9.0	–0.7
N15—N4—N5—C3	180.0	164.1	180.0	131.1	123.0
O7—C1—C2—N5	180.0	–179.8	180.0	–173.0	180.0
O8—C1—C2—N5	180.0	–0.8	180.0	7.3	–174.7
O10—C2—C3—C1	–145.5	143.1	–145.7	–150.8	–142.8
O11—C2—C3—C1	145.6	–149.8	145.7	140.4	148.2
O13—C3—N4—C2	180.0	178.5	180.0	165.2	–171.0
O14—C3—N4—C2	180.0	–170.0	180.0	176.7	177.2
H16—N15—N4—N5		138.0	119.6	78.5	38.2
H17—N15—N4—N5		18.0		–100.8	
H18—C15—N4—N5			0		

---

[a] Lengths are in Angstroms. Angles are in degrees.

Table 2

The lowest frequencies (ω_L), *electronic energies* (E_0), *zero-point energies* (ZPE), *and thermal correction to enthalpy* (H_T) *of model molecules*

Compd	ω_L, cm^{-1}	E_0, a.u.	ZPE, a.u.	H_T, a.u.	Compd	ω_L, cm^{-1}	E_0, a.u.	ZPE, a.u.	H_T, a.u.
P20	31.7295	–914.9553671	0.081000	0.094517	**P23**	36.1329	–1119.4238387	0.081237	0.097765
P21	35.0205	–970.2845909	0.097467	0.112399	**P24**	26.2821	–1044.2396462	0.075751	0.091850
P22	31.2280	–954.2714586	0.108949	0.124082					

in **P23** are 1.442 Å, 1.472 Å, 1.434 Å, and 1.596 Å respectively. However, the O14···N15 distance in 1-nitroso-3,4,5-trinitropyrazole-2-oxide (**P24**) is 3.241 Å, which is the N···O-type interaction. The interatomic O7···O11 and O13···O10 distances in **P24** are 3.182 Å and 3.320 Å respectively. The bond lengths of C1—NO_2, C2—NO_2, C3—NO_2, and N4—NO are 1.437 Å, 1.468 Å, 1.438 Å, and 1.602 Å respectively. The N5—O_∞ lengths in **P20**, **P21**, **P22**, **P23** and **P24** are 1.236 Å, 1.247 Å, 1.240 Å, 1.230 Å, and 1.250 Å respectively. The C—NO_2 bond lengths indicate that the C2—NO_2 one is longer in **P23** than that in **P24**, **P20**, **P21**, and **P22** compounds. The lowest frequency, electronic energy, zero-point energy, and thermal correction to the enthalpy of the molecules are presented in Table 2. The frequency varying from 31.2280 cm^{-1} to 36.1330 cm^{-1} is known for NO_2 torsions, while 26.2821 cm^{-1} is for the N—O stretching of the NO group in the **P24** molecule.

Chemical energy of detonation. The calculated chemical energies (Q) of detonation of **P20**, **P21**, **P22, P23**, and **P24** are 1.56 kcal/g, 1.71 kcal/g, 1.37 kcal/g, 1.17 kcal/g, and 1.32 kcal/g respectively. From Table 4, it is seen that Q values are higher when compared to those for 3,4,5-trinitropyrazole and 1-amino-3,4,5-trinitropyrazole that are devoid of N-oxide bonds [3]. The chemical energy of detonation is related to the nature of substituent at N4-position as well as the strength of N-oxide bond. The Q value is inncreased as the NO_2 group at the amino hydrogen position of **P23** is substituted by NH_2 (**P21**), CH_3 (**P22**), and NO groups (**P24**). The model compound **P21** has higher Q value and **P23** has lower Q value. The presence of NO groups rather NO_2 group at N4-position appearing to be promising as the NO group enhanced the Q value by ~0.15 kcal/g more in **P24** molecule.

Crystal density. The optimized molecular structures of **P20**, **P21**, **P22**, **P23**, and **P24** computed at the B3LYP/aug-cc-pVDZ level have been used to determine the crystal densities with the Material Studio 4.1 package with the cvff force field and the Ewald summation method [19]. This approach is based on the generation of possible packing arrangements in all reasonable space groups and the search for low lying minima in the lattice energy surface. Generally, most of the organic compounds pack in $C2/c$, $P2_1$, $P2_1/c$, $P2_12_12_1$ and P-1, $Pbca$, $Pbcn$, $Pna2_1$, CC and/or $C2$ space groups [7]. The calculated lowest energy crystal characteristics of pyrazole and the designed compounds are presented in Table 3. The calculated crystal densities of the **P20**, **P21**, **P22**, **P23,** and **P24** compounds are 2.40 g/cm^3, 2.34 g/cm^3, 2.21 g/cm^3, 2.50 g/cm^3, and 2.42 g/cm^3 respectively. Pyrazole, **P21**, and **P22** have been packed in $P2_1/c$; **P20** is packed in $Pbca$; **P23** is packed in $P2_1$; and **P24** is packed in $Pna2_1$. The NH_2 or CH_3 group substitution at the N4-position of **P20** decreases the crystal density as compared to that of **P20**, **P21**, and **P23**. The crystal structures of the **P20**, **P21**, **P22**, and **P23** model compounds are presented in Fig. 2. The errors in the calculated densities are expected to be less than 0.03 g/cm^3 [23, 24], and thus, are fairly good to evaluate the detonation properties. The increased densities are presumably due to the intramolecular hydrogen bonds, as well as the layered structures in the crystal lattice.

Detonation performance. The performance properties of the designed compounds along with the experimental values of RDX, HMX, CL-20, and ONC are presented in Table 4. For RDX, HMX, CL-20. and ONC the experimental values of D and P are 8.75 km/s, 8.96 km/s, 9.40 km/s, 9.80 km/s and 34.70 GPa, 35.96 GPa, 42.0 GPa, 50.0 GPa respectively [7, 25]. Furthermore, at the B3LYP/aug-cc-pVDZ level, the calculated D and P of RDX and HMX are found to be 8.86 km/s, 9.10 km/s and 34.23 GPa, 39.40 GPa respectively. The values of D and P of **P20** (D 10.75 km/s and P 59.84 GPa),

Table 3

Calculated crystal characteristics of pyrazole and the title compounds

Compd	Cell volume, Å^3	Total energy, kJ/mol	Space group	Crystal system	*a*, *b*, *c*, Å α, β, γ, deg.	Density, g/cm^3
Pyrazole	363.609	0.9649	$P2_1/c$	monoclinic	4.97, 7.70, 10.45 α = γ = 90; β = 114.6	1.24
P20	1217.402	–747.164	*Pbca*	rhombic	11.72, 9.70, 10.72 α = β = γ = 90	2.40
P21	665.845	–684.136	$P2_1/c$	monoclinic	5.94, 10.11, 12.70 α = γ = 90, β = 119.13	2.34
P22	702.230	–674.888	$P2_1/c$	monoclinic	6.07, 10.14, 13.34 α = γ = 90, β = 21.06	2.21
P23	350.154	–885.854	$P2_1$	monoclinic	8.57, 8.18, 6.31 α = γ = 90, β = 52.18	2.50
P24	646.268	–375.450	$Pna2_1$	rhombic	8.08, 8.61, 9.30 α = β = γ = 90	2.42

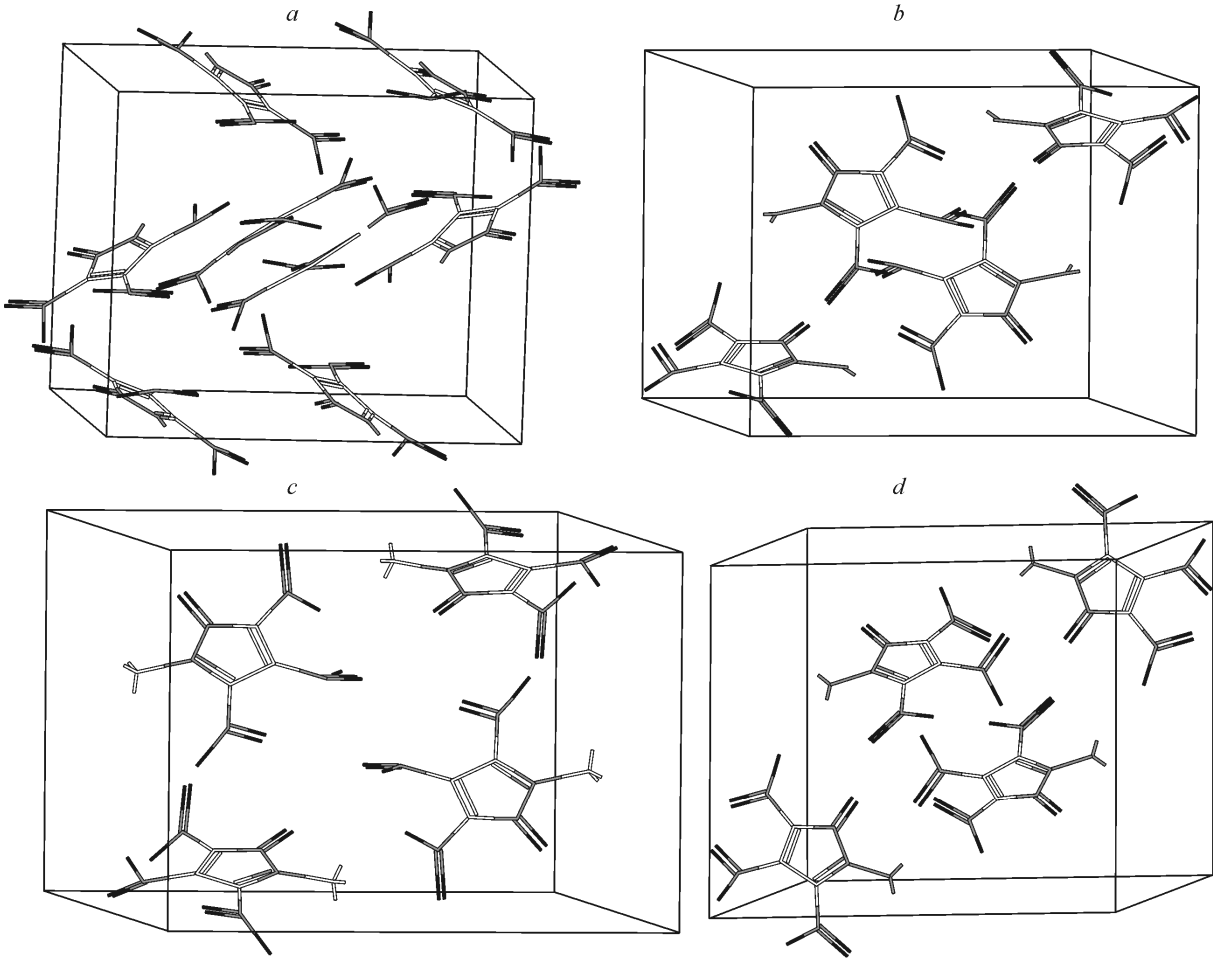

Fig. 2. Crystal structures of model compounds: (*a*) **P20**, (*b*) **P21**, (*c*) **P22**, and (*d*) **P23**

Table 4

Density (ρ), *energy of explosion* (Q), *detonation velocity* (D) *and detonation pressure* (P) *of model compounds*, RDX, HMX, CL-20 *and* ONC

Property	**P20**	**P21**	**P22**	**P23**	**P24**	RDX	HMX	CL-20	ONC
Mw	219	234	233	264	248	222	296	438	464
OB, %	+10.96	+10.26	+3.43	+18.18	+12.90	–25.80	–21.62	–11.0	0
ρ, g/cm^3	2.40	2.34	2.21	2.50	2.42	1.82	1.92	2.04	2.10
Q, kcal/g	1.56	1.71	1.37	1.17	1.32	1.27	1.27	1.85	2.20
D, km/s	10.75	10.92	10.26	10.27	10.36	8.75	8.96	9.38	9.80
P, GPa	59.84	61.04	52.31	55.74	55.80	34.70	35.96	42.0	50.00

P21 (D 10.92 km/s and P 61.04 GPa), **P22** (D 10.26 km/s and P 53.30 GPa), **P23** (D 10.27 km/s and P 55.74 GPa), and **P24** (D 10.36 km/s and P 55.80 GPa) appear to be promising compared with RDX, HMX, CL-20 and ONC. The higher performance properties of **P20** and **P21** are probably due to their positive oxygen balance (+10.96 % and +10.26 % respectively) and higher densities (2.40 g/cm^3 and 2.34 g/cm^3 respectively). Overall, the performance properties of the model molecules are higher compared to those of the known explosive compounds to the date.

Frontier molecular orbital energies. The frontier molecular orbital energies and their gaps of model compounds are presented in Table 5. Fukui et al. [17] noticed the prominent role played by the highest occupied molecular orbital (HOMO) and the lowest unoccupied molecular orbital (LUMO) in governing the chemical reactions of the compounds. It is known that the band gap $\Delta E_{(\text{LUMO—HOMO})}$ between LUMO and HOMO is an important stability index of the molecules [7, 17]. The smaller the band gap between HOMO and LUMO, the easier the electron transition and the lesser the stability of the explosive are. The LUMO energies vary from –0.15172 a.u. to –0.21632 a.u. and HOMO energies

Table 5

The nitro group charge ($-Q_{NO_2}$), *mid-point electrostatic potential* (V_{mid}), *electric spark sensitivity* (E_{ES}) *and frontier orbital energies of model compounds*

Compd	Bond	Length, Å	$-Q_{NO_2}$	V_{mid}	E_{ES}, J	HOMO, a.u.	LUMO, a.u.	$\Delta E_{\text{LUMO—HOMO}}$, a.u.
P20	C1—N6	1.440	0.533	1.865	12.21	–0.30236	–0.16090	0.14146
	C2—N9	1.470	0.742	2.054	12.34			
	C3—N12	1.427	0.570	1.861	10.60			
P21	C1—N6	1.438	0.545	1.826	10.16	–0.29483	–0.15483	0.14000
	C2—N9	1.470	0.740	1.988	12.14			
	C3—N12	1.427	0.590	1.636	10.62			
P22	C1—N6	1.440	0.537	1.733	10.00	–0.29307	–0.15172	0.14135
	C2—N9	1.470	0.718	1.913	12.83			
	C3—N12	1.433	0.597	1.664	10.60			
P23	C1—N6	1.442	0.525	1.980	10.80	–0.31415	–0.18387	0.13028
	C2—N9	1.472	0.706	1.923	12.63			
	C3—N12	1.434	0.597	2.137	11.57			
	N4—N15	1.596	0.081	0.906	6.28			
P24	C1—N6	1.437	0.552	1.912	12.00	–0.29350	–0.21632	0.07718
	C2—N9	1.468	0.726	1.968	13.76			
	C3—N12	1.438	0.622	1.893	12.70			
	N4—N15	1.602	0.412	0.100	2.40			

vary from –0.2937 a.u. to –0.31415 a.u. for the compounds. The frontier orbital energy gap varies from 0.07718 a.u. to 0.14146 a.u., and hence, the model compounds are stable. As for the designed compounds, the band gap of **P20** is the largest (0.14146 a.u.) and is the smallest (0.07718 a.u.) for **P24**, indicating that the former is more stable than the later. However, the **P23** molecule (0.13028 a.u.) shows a higher band gap compared to that of the **P24** molecule. Compounds **P20**, **P21**, and **P22** appear to be more stable, and the stability here refers to the chemical or photochemical processes with electron transfer or electron leap. Therefore, the decreasing order of stability is as follows: **P20** > **P22** > **P21** > **P23** > **P24**. Moreover, C—NO_2, N—NO_2, and N—NO are the trigger bonds in these compounds, and the resonance in the pyrazole ring strengthens these linkages, thereby the molecules get stabilized. The larger the length of trigger bonds of the molecule, the easier the dissociation or breakdown is, thus the molecule becomes lesser stable.

Impact sensitivity correlations. The impact sensitivity ($H_{50\,\%}$) is measured by the height, from where a given weight falling upon an explosive compound gives a 50 % probability of initiating an explosion. As for the NO_2 group in nitro compounds, they are electron-withdrawing. The higher the negative charge of the nitro group, the lower the electron withdrawing ability is, and therefore the more stable the nitro compound is. In explosives, C—NO_2, N—NO_2, and O—NO_2 bonds denoted as the R—NO_2 bond are usually the weakest in the molecule and their breaking is often the initial step in the decomposition or detonation. Normally, the charge on the nitro group ($—Q_{NO_2}$) is calculated by the sum of the net Mulliken atomic charges on the nitrogen (Q_N) and oxygen atoms (Q_{O1} and Q_{O2}) in the nitro group.

$$—Q_{NO_2} = Q_N + Q_{O_1} + Q_{O_2}. \tag{9}$$

The higher $—Q_{NO_2}$ is, the larger the impact insensitivity, and hence $—Q_{NO_2}$ is regarded as the criterion for estimating the impact sensitivities. Calculated $—Q_{NO_2}$ for the model compounds vary from 0.412 e to 0.712 e. The C1—NO_2 bonds in **P20**, **P21**, and **P22** are the site of shock initiation. The computed nitro group charge, midpoint electrostatic potential, trigger bond lengths of the molecules are presented in Table 5. The $—Q_{NO_2}$ values in **P20**, **P21**, and **P22** are 0.533 e, 0.545 e, and 0.537 e respectively. As per predicted by Zhang et al. [11, 12], these values are higher with respect to TNT (0.249 e), FOX-7 (0.365 e), RDX (0.134 e), HMX (0.112 e), TNAZ (0.114 e), LLM-105 (0.292 e), NTO (0.264 e), DNPP (0.305 e), CL-20 (0.081 e), ONC (0.146 e) and are found to be more insensitive. The presence of NH_2 and CH_3 groups at the N4-position increases the impact sensitivity. The impact sensitivity of **P23** appears to be as similar as ONC with the nitro group charge of 0.081, and **P24** is highly sensitive. It is also the same for the midpoint electrostatic potential (V_{mid}) values. Compound **P20** has the highest V_{mid} value (1.865), while compound **R24** has lowest $—Q_{NO_2}$ value (0.100). The stability here may be attributed to the presence of the π-excessive aromatic heterocyclic ring, the delocalization of π-electrons, and the presence of a new type of intramolecular N—H···O and N···O interactions.

Electric spark sensitivity correlations. Electric spark sensitivity is the degree of sensitivity of the energetic compound to the electric discharge. It is usually determined by subjecting the explosive compound to a high-voltage discharge from the capacitor. Zeman [13, 14] gave the relationship between the electric spark sensitivity (E_{ES}), the squares of detonation velocity (D), reciprocal temperatures, the Piloyan activation energy, and the heats of fusion of the energetic compounds. Wang et al. [16] gave a suitable correlation between the electric spark sensitivity, detonation velocity, and detonation pressure of nitramines and nitroarenes. We have calculated the electric spark sensitivity of the model compounds using the better correlation proposed by Zhi et al. [15]

$$E_{ES}(J) = (-1)^{n1} 10.16\, Q_{NO_2} - 1.05_{n1\ n2} E_{LUMO} - 0.20 \tag{10}$$

where, $n1$ is the number of aromatic rings, $n2$ is the number of substituted groups attached to the aromatic ring such as alkyl (—R) or amino (—NH_2) groups, $—Q_{NO_2}$ is the minimum Milliken charges of the NO_2 group, and E_{LUMO} (in eV) is the LUMO energy. As per calculated by Zhi et al. [15], the calculated electric spark sensitivity values of compounds **P20** (10.60 J), **P21** (10.16 J), and **P22** (10.00 J) are higher compared with that of TNT (6.94 J); however, the spark sensitivity of **P23** (6.30 J) is nearly equal to that of TNT.

CONCLUSIONS

In conclusion, the geometry, band gap, crystal density, detonation properties of the model molecules have been explored at the B3LYP/aug-cc-pVDZ level of calculation. The calculated detonation energies of **P20**, **P21**, **P22, P23**, and **P24** are 203.2 kJ/mol, 256.4 kJ/mol, 220.1 kJ/mol, and 279.2 kJ/mol respectively. The crystal densities of **P20**, **P21**, **P22**, **P23**, and **P24** are 2.40 g/cm^3, 2.34 g/cm^3, 2.21 g/cm^3, 2.50 g/cm^3, and 2.42 g/cm^3 respectively. The values of D and P of **P20** (D 10.75 km/s and P 59.84 GPa), **P21** (D 10.92 km/s and P 61.04 GPa), **P22** (D 10.26 km/s and P 53.30 GPa), **P23** (D 10.27 km/s and P 55.74 GPa), and **P24** (D 10.36 km/s and P 55.80 GPa) appear to be promising compared to those of RDX, HMX, CL-20 and ONC.

Acknowledgements. We are very grateful to the referees for their useful comments. The first author acknowledges the sustaining financial support from the Defence Research Development Organization (DRDO), India through the Advanced Centre of Research in High Energy Materials (ACRHEM).

REFERENCES

1. *Zaitsev A.A., Dalinger I.L., Shevelev S.A.* // Russ. Chem. Rev. – 2009. – **78**. – P. 589 – 627.
2. *Janssen J.W.A.M., Koeners H.J., Kruse C.G., Habraken C.L.* // J. Org. Chem. – 1973. – **38**. – P. 1777 – 1782.
3. *Herve G., Roussel C., Graindorg H.* // Angew Chem. Int. Ed. – 2010. – **49**. – P. 3177 – 3181.
4. *Dalinger I.L., Cherkasova T.I., Popova G.P., Shkineva T.K., Vatsadze I.A., Shevelev S.A., Kanishchev M.I.* // Russ. Chem. Bull. Int.Ed. – 2009. – **58**. – P. 410 – 413.
5. *Dalinger I.L., Popova G.P., Vatsadze I.A., Shkineva T.K., Shevelev S.A.* // Russ. Chem. Bull. Int. Ed. – 2009. – **58**. – P. 2185.
6. *Dalinger I.L., Vatsadze I.A., Shkineva T.K., Popova G.P., Shevelev S.A.* // Mendeleev Commun. – 2000. – **20**. – P. 253 – 254.
7. *Pinkerton A.A., Zhuorva E.A., Chen Y.-S.* In: P. Politzer, J.S. Murray (Eds.) Energetic Materials, Theoretical and Computational Chemistry Series. – New York: Elsevier, 2003.
8. *Murray J.S., Concha M.C., Politzer P.* // Mol. Phys. – 2009. – **107**. – P. 89 – 97.
9. *Rice B.M., Hare J.J.* // J. Phys. Chem. A. – 2002. – **106**. – P. 1770 – 1783.
10. *Pospìŝil M., Vávra P., Concha M.C., Murray J.S., Politzer P.* // J. Mol. Model. – 2010. – **16**. – P. 895 – 901.
11. *Zhang C., Shu Y., Huang Y., Zhao X., Dong H.* // J. Phys. Chem. B. – 2005. – **109**. – P. 8978 – 8982.
12. *Zhang C.* // J. Hazard. Mater. – 2009. – **161**. – P. 21 – 28.
13. *Zeman S.* // J. Energetic. Mater. – 1999. – **17**. – P. 305 – 329.
14. *Zeman S.* // J. Hazard. Mater. – 2006. – **132**. – P. 155 – 164.
15. *Zhi C., Cheng X.* // Propellants Explos, Pyretech. – 2010. – **35**. – P. 555 – 560.
16. *Wang G., Xiao H., Ju X., Gong X.* // Propellants Explos., Pyretech. – 2006. – **2**. – P. 102 – 109.
17. *Fukui F., Yonezawa T., Shingu H.* // J. Chem. Phys. – 1952. – **20**. – P. 722 – 725.
18. *Frisch M.J. et al.* Gaussian 03, Revision B.04, Gaussian, Inc., Pittsburgh PA. 2003.
19. *Materials* Studio version 4.1, Accelrys Inc., San Diego, CA, 2004.
20. *Kamlet M.J., Jacobs S.J.* // J. Chem. Phys. – 1968. – **48**. – P. 23 – 25.
21. *Akhavan J.* // Chemistry of Explosives, The Royal Society of Chemistry, Cambridge, 1998.
22. *Desiraju G.R., Steiner T.* // The Weak Hydrogen Bond. – New York: Oxford University Press, 1999.
23. *Kim J.K., Cho S.G, Kim C.K., Park H.-Y., Zhang H., Lee H.W.* // J. Compu. Chem. – 2008. – **29**. – P. 1818 – 1824.
24. *Politzer P., Martinez J., Murray J.S., Concha M.C., Alejandro T.-B.* // Mol. Phys. – 2009. – **107**. – P. 2095 – 2101.
25. *Pagoria P.F., Lee J.S., Mitchell A.R., Schmidt R.D.* // Thermochim. Acta. – 2002. – **384**. – P. 187 – 204.